Environmental Health Engineering and Management Journal 2024, 11(3), 361-370
http://ehemj.com
doi 10.34172/EHEM.2024.35

Environmental Health Engineering and Management Journal

Original Article

Environmental Health Engineering and Management

Open Access Publish Free

Innovative biofiltration materials for H2S removal from biogas

Kamyab Mohammadi*, Rasa Vaiskunaite, Alvydas Zagorskis

Department of Environment and Water Engineering, Faculty of Environmental Protection Technology and Management, Vilnius Tech University, Vilnius, Lithuania

Abstract

Background: Following an extensive examination of various biofiltration packing materials within a typical bioreactor (a biofilter) is aiming to remove hydrogen sulfide (H_2S) in the raw biogas.

Methods: Both biochar (pre- and post-pyrolysis at 400, 500, and 600 °C) and cellular concrete (CLC) waste, representing organic and inorganic packing materials, respectively, displayed remarkable removal efficiency (RE) performance under dynamic conditions. Nevertheless, the physical and chemical properties of these packing materials play a crucial role in absorbing and trapping H_2S for further filtration from the raw biogas. Key evaluations encompass chemical compositions, porosity, and specific surface area, aligning with contemporary research methodologies (e.g., XRF, Walkley-black, Kjeldahl, BET, T-plot), as analyzed in this study.

Results: Subsequently, the modification of these physicochemical properties aimed to demonstrate continued interactions of iron (III) oxide (Fe_2O_3) with H_2S for chemical modification of CLC waste, and enhance the specific surface area of biochar from 12, 22, and 24 m^2/g to 235, 433, 475 m^2/g, and for porosity from 0.01, 0.42, and 0.025 cm^3/g to 0.096, 4, 0.24 cm^3/g, respectively, for physical modification of biochar samples after pyrolysis at 400, 500, and 600 °C.

Conclusion: In the end, improving the possibility of getting better RE from a laboratory-scale biofilter is possible by modification of the most effective physical (adding KOH to biochar and increasing porosity by 9 times, specific surface area by 19 times) and chemical (adding Fe_2O_3 to CLC waste) properties of the environment-friendly packing materials.

Keywords: Bioreactors, Hydrogen sulfide, Biofuel, Biochar, Pyrolysis

Citation: Mohammadi K, Vaiskunaite R, Zagorskis A. Innovative biofiltration materials for H2S removal from biogas. Environmental Health Engineering and Management Journal 2024; 11(3): 361-370 doi: 10.34172/EHEM.2024.35.

Article History:
Received: 20 May 2024
Accepted: 24 June 2024
ePublished: 6 September 2024

***Correspondence to:**
Kamyab Mohammadi,
Email: kamyab.mohammadi@vilniustech.lt

Introduction

Toxic hydrogen sulfide (H_2S) found in raw biogas is very harmful to the environment and human health (1-4). It must be removed before using biogas to generate electricity (5). There are different ways to clean H_2S from biogas. Biofilters are one of the effective methods (5,6). The materials used in these filters are important because they affect how efficiently the filter works, how long it lasts, and the conditions needed to accurately evaluate removal efficiency (RE) (3,5). In the biofiltration method, a mix of organic or inorganic materials is used to separate H_2S from biogas (7,8). The best packing materials have high porosity to trap H_2S, a big surface area for chemical interactions, and contain specific heavy metals like iron, potassium, or calcium (9,10). This study aimed to find the best eco-friendly packing materials, understand what makes them unique, measure and improve their physicochemical properties, and make them better at cleaning H_2S from biogas. Using biochar in anaerobic digesters helps manage the end-life of agricultural waste and raises soil fertility by recovering sulfur trapped in H_2S (11,12). Biochar is made from heating biomass or organic waste in the situation of lack of oxygen and is usually born below 700 °C (13-15). It can come from different sources like rice husks (hulls), camphor, or bamboo (both woods of specific trees) (16-18). Because biochar has a large surface area and can trap ions, it's highly recommended for removing pollutants (19-21). Biochar's ability to absorb and oxidize H_2S is because of the presence of oxygen groups in its structure (22). Research on biochar from various sources shows that its alkaline nature helps remove H_2S by making it easier to react with other compounds (22). Biochar is a cost-effective way to clean because it can be made from different waste materials. Its high pH buffering capacity, due to the presence of sodium, potassium, calcium, and magnesium, is beneficial (22,23). When biochar is used, it can aid in the growth and function of methane-producing bacteria. This was a specific suggestion proposed by other researchers (24,25). Studies found that biochar modified with magnetite can remove over 90% of H_2S while adding

it to compost or reactors can greatly reduce H_2S levels without affecting other processes (26) (Figure 1). The effectiveness of a biofilter in cleaning H_2S was also tested using waste from cellular concrete (CLC) as the packing material (Figure 2). The study found that removing H_2S was successfully almost done in moist scenarios (2,5). When the H_2S concentration was 50 parts per million (ppm) and the empty bed retention time was 56 seconds, the RE was between 90 to 95% reported by Danila et al (9). The creation of gypsum was mainly due to reactions between H_2S and calcium carbonate ($CaCO_3$) in CLC waste reported by Ying et al (27).

Generally, there are two main obstacles to biologically eliminating H_2S from biogas, which were reported in many relevant articles (11,13). Slow reaction rates: Biological processes are generally slower than chemical reactions, which can be a limitation in systems requiring rapid H_2S removal (14,16). One of the main reasons raised this issue is the lack of sufficient porosity and specific surface area to give enough space to sulfur-oxidizing bacteria living in the packing bed of the biofilter, to engage in the desulfurization process (23,39). Sensitivity to environmental conditions: Sulfur-oxidizing bacteria are too sensitive to different environmental factors and eventually negatively impact the performance of biofilters (14,16). By amplifying chemical interactions in the packing materials that help the desulfurization process of H_2S, apart from those done by these microorganisms, the ultimate RE of the biofilter will be raised even further. The main goal of this study was to examine the important chemical and physical properties (like composition, porosity, and surface area) of selected packing materials for biofilters (biochar and CLC waste), and by modifying these physicochemical properties, reach even higher RE.

Materials and Methods

In this study, sludge from the Vilnius sewage treatment plant separately went into two different processing methods: Immediate drying under 100 °C, or after pyrolysis at 400, 500, and 600 °C. Immediate dried sludge from composting needs preparation, which involves grinding to reduce size (make them more convenient before sifting). However, sludge from the thermal bioreactor can be directly prepared for pyrolysis at different temperatures (under 700 °C) (14,20,22-27). CLC has a much lower density compared to regular concrete (2400 kg/m^3 > 400-1000 kg/m^3). Foam replaces stone aggregates in CLC. Hence, it would be structured from cement, sand, foam, and water (16,26-28). In our case study, even sand was omitted to achieve the lowest possible density and avoid unnecessary compaction in the biofilter. The CLC waste sample used in this work has an 11 mm thickness. All analysis methods were taken from the "Standard Methods for Examination of Water and Wastewater, 20th edition (28).

To determine nitrogen content in biochar, the Kjeldahl method is used according to the clean air act (CAA) standards (29-31). In this method, biochar samples are mixed with a solution of sulfuric acid, to convert nitrogen to ammonium sulfate. Then, nitrogen is converted into ammonia and further into ammonium borate. Nitrogen amount is determined by titration with consumed acid (10,19,32,33). The Walkley-Black method is used to determine the organic carbon content of the biochar

Figure 2. CLC waste used in this study under compressive strength examination

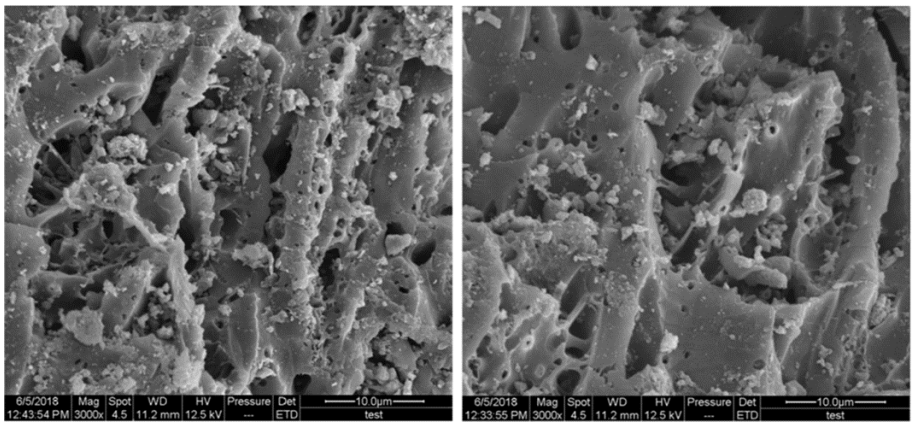

Figure 1. Schematic of the biochar sample (in 10 µm scale) before (left) and after (right) biofiltering H_2S from biogas (27)

samples, following again the CAA standards (16,26,34). Organic carbon in the samples is oxidized using a 0.167 M solution of potassium dichromate ($K_2Cr_2O_7$) in concentrated sulfuric acid (2,9,17,35). The reaction is quite intense and raises the temperature enough to make significant oxidation. The spectrophotometry method further measures the remaining chromate at a wavelength of 600 nanometers (nm) (5,28,29,36). Both assessments were carried out in the Chemistry Laboratory at Ferdowsi University, Iran. The X-ray fluorescence (XRF) method involves exposing the biochar and CLC waste samples to radiation generated by an X-ray tube (7,8,37). The tool used for this technique is shown in Figure 3. Following the CAA standards, specific X-ray emission from the examined samples is compared to the initial samples from the calibration tests (7,8,37). This method determines concentrations of sulfur (S) and magnesium (Mg) in biochar samples, sulfur trioxide (SO_3) in CLC waste, and silicon (Si), calcium (Ca), aluminum (Al), phosphorus (P), iron (Fe), and potassium (K) in both packing materials (7,8,31). These concentrations are expressed as mass percentages. At least three calibration curves are needed to cover the concentration range from 0 to 100% mass percentages (7,8,37). This analysis was carried out in the Chemistry Laboratory at Ferdowsi University, Iran.

The T-plot method, instructed by the new source performance standards (NSPS), is a significant technique for determining small and mesoporous volumes of a sample (38,39). It involves accurately comparing the sample's adsorption isotherm with that of another nonporous material (low porosity) with a similar structure (38,39). This assessment was carried out in the Civil Engineering Laboratory at Tehran University in Iran. The total porosity of the measured samples was analyzed by equation 3 (38,39).

$$T(\text{nm}) = \left[13.99 / 0.034 - \log(R)\right] 1/2 \quad (1)$$

$$R = (P)/(P0) \quad (2)$$

Figure 3. X-ray fluorescence device to extract the chemical structure of the packing materials

$$\text{Porosity}(\%) = \left[\begin{array}{l}\text{Pores}(\text{total quantity adsorbed}) / \\ \text{Volume}(\text{total size of sample})\end{array}\right] \times 100 \quad (3)$$

By the NSPS, a typical gas adsorption (Q) of a sample is analyzed using the BET (Brunauer, Emmett, and Teller) theory, which besides having relative pressure (R), provides insight into the sample's specific surface area expressed in units of area per mass of sample (m^2/g) (25,40,41). The temperature of the investigation chamber was recorded as -196.898 °C. This analysis was conducted in the Structural Engineering Laboratory at Tehran University, Iran. The specific surface area can be calculated based on the relative pressure and amount adsorbed using equation 4 as follows (42-44):

$$\text{Specific surface area}(\text{SBET})(\text{m}^2/\text{g}) = \text{average}(\text{AVG})(1/[\text{Q}(\text{R}-1)]) \quad (4)$$

Results

The experimental results, typically derived from three repetitions of each experimental treatment, were presented as the mean ± standard deviation. Variance analysis was performed, with only values having a *P* value below 0.05 considered significant. An analysis of variance (ANOVA) was conducted to determine significant differences in the adsorption capacity of sewage sludge biochar based on pH or phosphate concentration (15,34). Below are the obtained results regarding the chemical composition of CLC waste demonstrated in Table 1 and for biochar samples illustrated in Table 2. The thickness of sifted biochar samples was analyzed (equation 1) and demonstrated in Table 3. Whereas the obtained data of the T-plot diagrams shown in Table 4, represents the relative pressure (P/P^0), which is calculated from the division of the absolute pressure (P) of the sample to saturation pressure (P^0) of the sample, ranging from 0 to

Table 1. Evaluated chemical composition of CLC waste sample by XRF method

Chemical compositions	Biochar 400 °C	Biochar 500 °C	Biochar 600 °C	Sewage sludge
SiO_2	25.67%	29.82%	30.27%	18.93%
CaO	17.45%	15.47%	15.80%	11.83%
Al_2O_3	5.23%	5.14%	5.39%	3.53%
P_2O_5	13.43%	13.78%	14.38%	9.51%
Fe_2O_3	6.38%	6.67%	6.60%	4.38%
K_2O	1.78%	1.70%	1.70%	1.39%
MgO	3.39%	3.39%	3.50%	2.34%
S	0.78%	0.85%	0.81%	0.96%
N	2.10%	2.80%	2.10%	4.20%
C	24.17%	19.60%	15.41%	30.83%

1 (equation 2).

Based on ASTM C830-00 standard procedure, the nitrogen gas atoms can pass through particles and into all pores, breaks, and surface unpleasantness, so the estimation tests the full tiny surface area of the packing materials, which is the definition of the relative pressure used as a parameter in this evaluation. For the CLC waste sample, the micropore volume is 0.0168644 $cm^3.g^{-1}$, the external surface area is 115.11 $m^2.g^{-1}$, and the correlation coefficient is 0.680022. The total porosity of the sample is 97%. For the sewage sludge sample, the micropore volume is 0.04864 $cm^3.g^{-1}$, the external surface area of the case is 15.1651 $m^2.g^{-1}$, and the correlation coefficient is 0.995093. The total porosity of the sample is 9%. For biochar samples after 400 °C pyrolysis, the micropore volume is 0.01065 $m^2.g^{-1}$, the external surface area of the case is 14.0743 $m^2.g^{-1}$, and the correlation coefficient is 0.995524. The total porosity of the sample is 32%. For biochar samples after 500°C pyrolysis, the micropore volume is 0.4222 $cm^3.g^{-1}$, the external surface area of the case is 14.8306 $m^2.g^{-1}$, and the correlation coefficient is 0.995526. The total porosity of the sample is 57%. For biochar samples after 600 °C pyrolysis, the micropore volume is 0.0257 $cm^3.g^{-1}$, the external surface area of the case is 23.7746 $m^2.g^{-1}$, and the correlation coefficient is 0.999221. The total porosity of the sample is 65%. Figure 4 represents the comparison between obtained results of implemented different packing material's porosity. In this case, the micropore area is not reported because the calculated external surface area is larger than the total surface area.

Based on ASTM C1069-09 standard procedure, for the case CLC waste sample, BET surface area is 44 ± 0.8

Table 2. The results of X-ray fluorescence, Kjeldahl, and Walkley-black strategy examination for the chemical structure of case samples

Name of chemical compositions	CLC waste
SiO_2	48.50%
CaO	26.60%
SO_3	18.50%
Al_2O_3	2.70%
P_2O_5	1.90%
Fe_2O_3	1.40%
K_2O	0.30%

Table 3. The related analyzed porosity was evaluated based on the statistical thickness of sewage sludge, biochar pyrolyzed at 400 °C, 500 °C, and 600 °C

Thickness	Sewage sludge (quantity adsorbed)	Biochar 400 °C (quantity adsorbed)	Biochar 500 °C (quantity adsorbed)	Biochar 600 °C (quantity adsorbed)
0.36162 nm	0.6613 cm^3/g	2.6351 cm^3/g	5.4634 cm^3/g	5.6821 cm^3/g
0.36244 nm	0.4182 cm^3/g	2.7467 cm^3/g	5.1897 cm^3/g	5.8896 cm^3/g
0.39120 nm	0.5268 cm^3/g	2.8930 cm^3/g	5.3136 cm^3/g	6.1481 cm^3/g
0.40253 nm	0.7584 cm^3/g	2.9756 cm^3/g	5.5781 cm^3/g	6.3248 cm^3/g
0.41914 nm	0.9206 cm^3/g	3.1043 cm^3/g	5.7263 cm^3/g	6.5673 cm^3/g
0.43584 nm	1.0868 cm^3/g	3.2436 cm^3/g	5.8802 cm^3/g	6.8235 cm^3/g
0.45218 nm	1.2692 cm^3/g	3.3947 cm^3/g	6.0354 cm^3/g	7.0861 cm^3/g
0.46837 nm	1.4631 cm^3/g	3.5898 cm^3/g	6.2065 cm^3/g	7.3537 cm^3/g
0.48457 nm	1.6596 cm^3/g	3.7757 cm^3/g	6.3808 cm^3/g	7.6389 cm^3/g

Table 4. The related analyzed specific surface area was evaluated based on the relative pressure and quantity adsorbed by sewage sludge, and biochar after 400 °C, 500 °C, and 600 °C pyrolysis

Relative pressure	Sewage sludge (1/[Q (R-1)])	Biochar 400°C (1/[Q (R-1)])	Biochar 500°C (1/[Q (R-1)])	Biochar 600°C (1/[Q (R-1)])
0.0552612 p/p°	-	-	0.008334 m^2/g	0.011086 m^2/g
0.0705125 p/p°	-	0.023613 m^2/g	0.011139 m^2/g	0.013822 m^2/g
0.0862460 p/p°	0.219522 m^2/g	0.033226 m^2/g	0.016586 m^2/g	0.016611 m^2/g
0.1064887 p/p°	0.224705 m^2/g	0.038487 m^2/g	0.019004 m^2/g	0.020236 m^2/g
0.1317700 p/p°	0.225927 m^2/g	0.045566 m^2/g	0.023483 m^2/g	0.024685 m^2/g
0.1479092 p/p°	0.229034 m^2/g	0.054538 m^2/g	0.026429 m^2/g	0.027445 m^2/g
0.1726996 p/p°	0.228910 m^2/g	0.060193 m^2/g	0.031068 m^2/g	0.031787 m^2/g
0.1981724 p/p°	0.226685 m^2/g	0.068834 m^2/g	0.035970 m^2/g	0.036221 m^2/g
0.2235598 p/p°	0.227474 m^2/g	0.077871 m^2/g	0.041971 m^2/g	0.040633 m^2/g
0.2488169 p/p°	0.226854 m^2/g	0.086129 m^2/g	0.047019 m^2/g	0.045043 m^2/g
0.2741812 p/p°	0.226384 m^2/g	0.092227 m^2/g	0.051207 m^2/g	0.049451 m^2/g
0.2992768 p/p	0.227491 m^2/g	0.100698 m^2/g	0.056486 m^2/g	0.053847 m^2/g

$m^2.g^{-1}$, with a correlation coefficient of 0.5581211. For the case study of sewage sludge sample, BET surface area is 17.9668 ± 0.7187 $m^2.g^{-1}$. And respective correlation coefficient is detected to be 0.5573119. However, the micropore surface area is approximately 2.9264 $m^2.g^{-1}$, which represents the value of the micrometer particle's surface area. For the case study of biochar sample after 400°C pyrolysis, the assessed BET surface area is 12.2872 $m^2.g^{-1}$ ± 0.1568 $m^2.g^{-1}$ with the respective correlation coefficient of around 0.9992624. However, the micropore surface area is approximately 11.3395 $m^2.g^{-1}$, representing the micrometer particle's surface area value. For the case study of biochar sample after 500 °C pyrolysis, the assessed BET surface area is 19.7620 ± 0.2212 $m^2.g^{-1}$, which is achieved from the average of the data obtained from equation 2.6, besides the evaluated correlation coefficient of around 0.9996445. However, the micropore surface area is approximately 20.3936 $m^2.g^{-1}$, representing the micrometer particle's surface area value. For the case study of biochar sample after 600 °C pyrolysis, the assessed BET surface area is 24.6682 ± 0.0325 $m^2.g^{-1}$, which is achieved from the average of the data obtained from equation 2.6, while the correlation coefficient was detected to be 0.9999914. However, the micropore surface area is approximately 18.4128 $m^2.g^{-1}$, which represents the value of the micrometer particle's surface area. Figure 5 represents the comparison between obtained results of implemented different packing material's specific surface area.

Table 5 shows the obtained results after the modification of biochar samples with KOH combination.

Discussion

As presented in Table 1, silicon dioxide (SiO_2) and CaO are the primary organic components of CLC waste. Like biochar samples, CLC waste contains SO_3, aluminum oxide (Al_2O_3), phosphorus pentoxide (P_2O_5), iron (III) oxide (Fe_2O_3), and a small amount of potassium oxide (K_2O) (Table 1). In the case of CLC waste, there is a chemical interaction between H_2S and $CaCO_3$ that results in the creation of calcium sulfate ($CaSO_4$), also known as gypsum, through subsequent chemical interactions (equations 5-9). These chemical interactions have been observed in previous studies (19,24,33). The dissolution of calcium oxides (CaO) and $CaCO_3$, along with the

Table 5. Modification of the biochar sample's specific surface area and porosity by adding potassium hydroxide (KOH)

Physical parameters	Initial S_{BET} and porosity	Modified S_{BET} and porosity
S_{BET} biochar after 400°C pyrolysis	12.28 m^2/g	235.32 m^2/g
S_{BET} biochar after 500°C pyrolysis	22.76 m^2/g	433.44 m^2/g
S_{BET} biochar after 600°C pyrolysis	24.66 m^2/g	471.54 m^2/g
Porosity $_{BET}$ biochar after 400°C pyrolysis	0.01 cm^3/g	0.096 cm^3/g
Porosity $_{BET}$ biochar after 500°C pyrolysis	0.42 cm^3/g	4.00 cm^3/g
Porosity $_{BET}$ biochar after 600°C pyrolysis	0.025 cm^3/g	0.24 cm^3/g

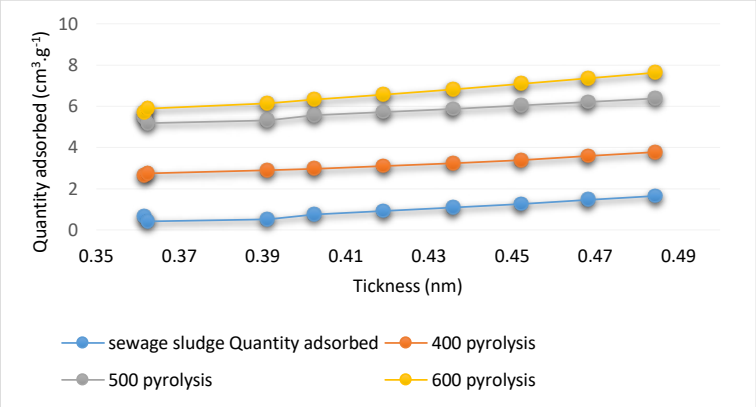

Figure 4. Porosity of sewage sludge, biochar pyrolyzed at 400 °C, 500 °C, and 600 °C. Samples based on thickness and quantity adsorbed

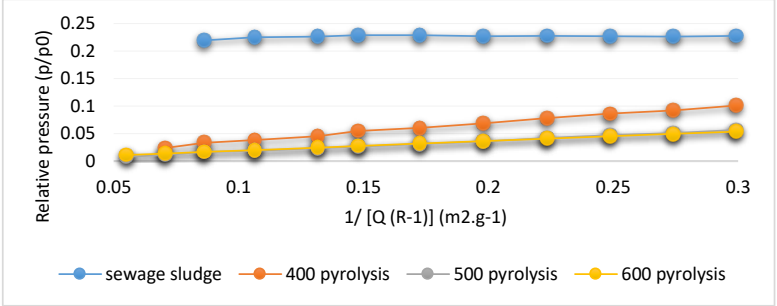

Figure 5. Comparison of specific surface area of sewage sludge, and biochar after 400 °C, 500 °C, and 600 °C pyrolysis samples

presence of $CaSO_4$, combines with the corrosion that is observed in major sewer pipelines due to H_2S formation in wastewater infrastructure systems.

$$CaO + H_2 \rightarrow CaS + H_2O \quad (5)$$

$$CaO + H_2O \rightarrow Ca(OH_2) \quad (6)$$

$$Ca(OH_2) + CO_2 \rightarrow CaCO_3 + H_2O \quad (7)$$

$$CaCO_3 + H_2S \rightarrow CaS + H_2O + CO_2 \quad (8)$$

$$CaS + 2CO_2 + 2H_2O \rightarrow CaSO_4 + H_2O + 2C \quad (9)$$

In Table 2, the nitrogen (N) and carbon (C) could not be analyzed using the XRF technique. Therefore, N and C were examined by implementing the Kjeldahl and Walkley-Black methods to obtain more accurate data regarding the chemical constituents in biochar samples. One aspect is the trend in organic carbon content analyzed using the Walkley-Black method for all biochar samples, which decreased in the following sequence (for pre-pyrolysis and after 400 °C, 500 °C, and 600 °C pyrolysis): 30%, 24%, 19%, 15%, respectively. Meanwhile, the percentage of nitrogen analyzed by the Kjeldahl method decreased by 2% from the beginning through the increase of the pyrolysis temperature for biochar samples. The percentages of sulfur (S) and potassium (K_2O) remained constant during pyrolysis. However, the percentages of CaO , Al_2O_3, P_2O_5, Fe_2O_3, and magnesium oxide (MgO) showed a significant increase after initial pyrolysis at 400 °C. Similar chemical composition of sewage sludge-derived biochar results were reported in previous studies (15,19,24). They also reported a reduction of carbon and nitrogen after the pyrolysis temperature of the biochar samples increased. In contrast to the rest of the chemical compositions, this same pattern is seen for SiO_2. This indicates that the proportion of silicon oxide increases as the percentages of N and C decrease at higher pyrolysis temperatures due to chemical interactions. The reduction in nitrogen and carbon by increasing pyrolysis temperature has been previously reported. Considering that Ca, Mg, and K are known to be the most active substances in absorbing and chemically interacting with H_2S, the percentages of these heavy metals remained consistent in the chemical structure of samples. Another consideration is the presence of N, as it is essential for the biofilter, and its presence must be controlled, especially if the decision is to use pyrolyzed biochar particles (400 °C/600 °C), requiring additional measures to increase nitrogen content. Nitrogen gas molecules can penetrate between particles and into all pores, cracks, and surface irregularities, so the assessment samples the full surface area of the packing materials, which is reflected in the relative pressure used as a parameter in this assessment.

As shown in Figure 4, which is drawn from the data presented in Table 3, the porosity gets bigger as the thickness grows for all sewage sludge, biochar pyrolyzed at 400 °C, 500 °C, and 600 °C samples, whereas the minimum acceptable porosity is 0.4182 achieved on 0.35663 nm thickness, and maximum acceptable porosity reached to 1.6596 nm on 0.48444 nm thickness, in the case of sewage sludge sample. The minimum acceptable porosity of 2.6351 was achieved on 0.36162 nm thickness, and the maximum acceptable porosity reached 3.7757 on 0.48534 nm thickness, in the case of biochar samples after 400 °C pyrolysis. The minimum acceptable porosity of 6.1897 was achieved on 0.36244 nm thickness, and the maximum acceptable porosity reached 7.3808 on 0.48457 nm thickness, in the case of biochar samples after 500 °C pyrolysis. The minimum acceptable porosity of 5.6821 was achieved on 0.35691 nm thickness, and the maximum acceptable porosity reached 7.6389 on 0.48451 nm thickness, in the case of biochar samples after 600 °C pyrolysis (35). Also, approximately similar porosities (61% and 71% for biochar samples pyrolyzed at 500 and 600 °C) were achieved (20). The same porosities were achieved for magnetic biochar particles pyrolyzed at 100, 200, and 300 °C (30%, 31%, 35%) (35).

Figure 5 drawn from the data presented in Table 4, represents a comparison between specific surface area for all sewage sludge, and biochar after 400, 500, and 600 °C pyrolysis samples. In the case of sewage sludge samples, data approximately followed the same amount during the whole experiment, relatively for lower and higher inserted pressure. There is a slight fluctuation in surface area at 0.07 (p/p°) to 0.15 (p/p°), but afterward, the area stabilized at 0.227 for the rest of the higher pressures till 0.25 (p/p°). Specific surface area for the biochar samples after 400 °C pyrolysis is approximately following the same enhancement line during the whole assessment, beginning from the 0.023 surface area at 0.05 relative pressure till 0.1 surface area captured at 0.275 relative pressure. The result indicates that as much as the relative pressure increases, the specific surface area for this case study will get bigger. Specific surface area for the biochar samples after 500 °C pyrolysis is approximately following the same increase line during the whole experiment, beginning from the 0.016 surface area at 0.09 relative pressure till 0.056 surface area captured at 0.3 relative pressure. The result indicates that as much as the relative pressure is enhanced, the specific surface area for this case study will get bigger. The specific surface area for the biochar samples after 600 °C pyrolysis is approximately following the same increase line during the whole assessment, beginning from the 0.011 surface area at 0.065 relative pressure till 0.054 surface area captured at 0.3 relative pressure. The result is somehow similar to the ones achieved for biochar samples after 500 °C pyrolysis, indicating as much as the relative pressure is

enhanced, the specific surface area for this case study will get bigger. González-Cortés et al (7) and Jiang et al (13) also presented 10 $m^2.g^{-1}$, 20 $m^2.g^{-1}$ specific surface area reached for biochar after pyrolysis at 330 °C and 380 °C.

Based on the data presented in Table 5, utilizing biochar samples after 500 °C pyrolysis is the most favorable option among the biochar samples after activation. They have nearly identical specific surface area to those after 600 °C pyrolysis (both exceeding 400 m^2/g) and significantly higher porosity (around 4 cm^3/g), compared to other biochar samples. Higher porosity gives sufficient space to the sulfur-oxidizing bacteria living in the packing material to trap separated forms of sulfur, sulfide, or sulfate into the packing material apart from re-engaging with hydrogen molecules. The study aimed to increase the specific surface area of biochar so that sulfur-oxidizing bacteria could participate more actively in the desulfurization process. Additionally, chemical compounds like SiO_2, Al_2O_3, and Fe_2O_3 present in the biochar samples contribute to H_2S purification from biogas, like CLC waste. The reactivity potential order hypothetically is $Fe_2O_3 > Al_2O_3 > SiO_2$. Considering the weight of Fe_2O_3 in CLC waste is 1.40%, it likely catalyzes reactions with H_2S. This suggests that biochar samples, especially those from pyrolysis at 500 °C, offer promising potential for efficient H_2S removal from biogas due to their favorable physical and chemical properties.

$$Fe_2O_3 + 3H_2S \rightarrow FE_2S_3 + 3H_2O \quad (10)$$

However, when there is sufficient temperature, catalysts, and pressure, the equations below will take place (11 and 12):

$$Fe_2S_3 \rightarrow FeS + FeS_2 \quad (11)$$

$$2(FeS_2) \rightarrow 2(FeS) + S_2 \quad (12)$$

If sufficient oxygen is provided into the biofilter, there would be further chemical interactions between H_2S and Fe_2O_3, as displayed in equation 13:

$$2(Fe_2S_3) + 9O_2 \rightarrow 2(Fe_2O_3) + 6(SO_2) \quad (13)$$

The primary goal of this work was to improve the biofilter efficiency by modifying the physical and chemical properties of the packing materials. By increasing their physical properties like specific surface area and porosity while ensuring durability and strength, we aimed to enhance packing material's EC and RE. Moreover, by carefully adjusting their chemical composition and adding specific chemical compounds, we could enhance their affinity, chemical interactions, and even further desulfurization of H_2S from biogas.

Conclusion

The study was dedicated to a comprehensive evaluation of the most effective environment-friendly packing materials (sewage sludge, biochar, polyurethane foam, and CLC waste) used for H_2S removal from biogas in a biofilter. Hence, the physicochemical properties (porosity, specific surface area, and chemical composition) of these materials were examined, and finally, the ways to improve these properties and eventually, the packing material's removal efficiency were identified.

1. The porosity of packing materials is crucial for trapping hydrogen sulfide (H_2S) and initiating desulfurization by microorganisms. Polyurethane foam CLC waste and biochar after 600°C pyrolysis had the highest porosity, reaching 64% and 65%, respectively. Conversely, biochar before pyrolysis showed the lowest porosity at 9%, but as pyrolysis temperature increased, porosity improved significantly, reaching 65% after pyrolysis at 600 °C.
2. Specific surface area of packing materials is vital for interacting with H_2S and microbial processes. CLC waste had the highest surface area at 44 m^2/g, while biochar after 400 °C pyrolysis had the lowest one at 12 m^2/g. Biochar surface area increased with pyrolysis temperature, reaching up to 24 m^2/g.
3. Chemical compositions of biochar and CLC waste were analyzed using various methods. CLC waste had significant Ca content (26.60%), suggesting potential chemical interactions with H_2S. Biochar samples showed decreased nitrogen and carbon with higher pyrolysis temperature, while elements like SiO_2, CaO, Al_2O_3, P_2O_5, and Fe_2O_3 became more prominent. Biochar after 600 °C pyrolysis had the highest heavy metal concentration, affecting chemical interaction rates with H_2S.
4. To modify packing materials' properties, controlled amounts of Fe_2O_3 were added to CLC waste to enhance desulfurization potential. KOH was added to biochar samples, especially after 600 °C pyrolysis, resulting in increased porosity (up to 0.24 cm^3/g) and specific surface area (up to 471 m^2/g).

However, as stated at the beginning of the research, this study concentrated on only reviewing the impact of porosity, specific surface area, and chemical composition of the sewage sludge-derived biochar and CLC waste, while still there are some other effective physicochemical parameters on packing materials performance to amplify desulfurization process of hydrogen sulfide from biogas such as pH, electrical conductivity, water retention capacity, oxygen content, etc. Monitoring and controlling these parameters, besides other environmental factors' impacts like temperature, humidity, flow rate, etc., are the main challenges and scientific deficiencies of this work that need to be addressed and considered in future investigations. As other researchers study biochar with potential properties of increased surface area distributed in different functional groups, with specific surface

morphology, etc., according to other researchers, the most important application of biochar is as an adsorbent to help remove various forms of water/air pollutants such as organic, inorganic pollutants, etc. Interactions of biochar with water/air pollutants are also being investigated to understand the interrelated mechanisms. In the future, more attention should be paid to research related to biochar dynamic adsorption systems, taking into account the multicomponent properties of pollutants. Furthermore, the aspect of disposal of the spent adsorbent from biochar-derived sewage sludge is one of the more insightful perspectives for future research to explore future desorption strategies.

Acknowledgments

This study was extracted from a doctoral dissertation conducted at the Vilnius Tech University. I would like to express my sincere gratitude to the faculty of Environmental and Water Engineering, for their invaluable contribution and support throughout the development of this article. Additionally, I extend my heartfelt appreciation to Prof. Rasa Vaiskunaite and Prof. Alvydas Zagorskis for their insightful discussions and constructive feedback, which have enriched the content of this article.

Authors' contributions

Conceptualization: Kamyab Mohammadi, Rasa Vaiskunaite.
Data curation: Kamyab Mohammadi.
Formal analysis: Kamyab Mohammadi, Rasa Vaiskunaite.
Funding acquisition: Rasa Vaiskunaite.
Investigation: Kamyab Mohammadi.
Methodology: Kamyab Mohammadi.
Project administration: Kamyab Mohammadi, Rasa Vaiskunaite.
Resources: Kamyab Mohammadi, Rasa Vaiskunaite.
Software: Kamyab Mohammadi.
Supervision: Rasa Vaiskunaite.
Validation: Kamyab Mohammadi, Rasa Vaiskunaite, Alvydas Zagorskis.
Visualization: Kamyab Mohammadi.
Writing–original draft: Kamyab Mohammadi.
Writing–review & editing: Kamyab Mohammadi, Rasa Vaiskunaite, Alvydas Zagorskis.

Competing interests

The author declares that he has no competing interests.

Ethical issues

The author hereby certifies that all data collected during the study are as stated in the manuscript, and no data from the study has been or will be published separately elsewhere.

Funding

The present scientific work was not funded by any individual or organization, which raises concerns about either approval or rejection of the article, after submission to the Environmental Health Engineering and Management journal.

References

1. Zhu HL, Papurello D, Gandiglio M, Lanzini A, Akpinar I, Shearing PR, et al. Study of H2S removal capability from simulated biogas by using waste-derived adsorbent materials. Processes. 2020;8(9):1030. doi: 10.3390/pr8091030.
2. Appala VN, Pandhare NN, Bajpai S. Mathematical models for optimization of anaerobic digestion and biogas production. In: Nandabalan YK, Garg VK, Labhsetwar NK, Singh A, eds. Zero Waste Biorefinery. Singapore: Springer; 2022. p. 575-91. doi: 10.1007/978-981-16-8682-5_21.
3. Xu Y, Chen Y, Ma C, Qiao W, Wang J, Ling L. Functionalization of activated carbon fiber mat with bimetallic active sites for NH3 and H2S adsorption at room temperature. Sep Purif Technol. 2022;303:122335. doi: 10.1016/j.seppur.2022.122335.
4. Vaiškūnaitė R. Cleaning of H2S from polluted air using peat biofilter. Moksl Liet Ateitis. 2020;12:1-5. doi: 10.3846/mla.2020.13081.
5. Cano PI, Almenglo F, Ramírez M, Cantero D. Integration of a nitrification bioreactor and an anoxic biotrickling filter for simultaneous ammonium-rich water treatment and biogas desulfurization. Chemosphere. 2021;284:131358. doi: 10.1016/j.chemosphere.2021.131358.
6. Watsuntorn W, Khanongnuch R, Chulalaksananukul W, Rene ER, Lens PN. Resilient performance of an anoxic biotrickling filter for hydrogen sulphide removal from a biogas mimic: steady, transient state and neural network evaluation. J Clean Prod. 2020;249:119351. doi: 10.1016/j.jclepro.2019.119351.
7. González-Cortés JJ, Almenglo F, Ramírez M, Cantero D. Simultaneous removal of ammonium from landfill leachate and hydrogen sulfide from biogas using a novel two-stage oxic-anoxic system. Sci Total Environ. 2021;750:141664. doi: 10.1016/j.scitotenv.2020.141664.
8. Khan MU, Lee JT, Bashir MA, Dissanayake PD, Ok YS, Tong YW, et al. Current status of biogas upgrading for direct biomethane use: a review. Renew Sustain Energy Rev. 2021;149:111343. doi: 10.1016/j.rser.2021.111343.
9. Danila V, Zagorskis A, Januševičius T. Effects of water content and irrigation of packing materials on the performance of biofilters and biotrickling filters: a review. Processes. 2022;10(7):1304. doi: 10.3390/pr10071304.
10. de Souza FM, Kahol PK, Gupta RK. Introduction to Polyurethane Chemistry. In: Polyurethane Chemistry: Renewable Polyols and Isocyanates. American Chemical Society; 2021. p. 1-24. doi: 10.1021/bk-2021-1380.ch001.
11. Ghimire A, Gyawali R, Lens PN, Lohani SP. Technologies for removal of hydrogen sulfide (H2S) from biogas. In: Aryal N, Mørck Ottosen LD, Wegener Kofoed MV, Pant D, eds. Emerging Technologies and Biological Systems for Biogas Upgrading. Academic Press; 2021. p. 295-320. doi: 10.1016/b978-0-12-822808-1.00011-8.
12. Haosagul S, Prommeenate P, Hobbs G, Pisutpaisal N. Sulfur-oxidizing bacteria in full-scale biogas cleanup system of ethanol industry. Renew Energy. 2020;150:965-72. doi: 10.1016/j.renene.2019.11.140.

13. Jiang X, Wu J, Jin Z, Yang S, Shen L. Enhancing the removal of H2S from biogas through refluxing of outlet gas in biological bubble-column. Bioresour Technol. 2020;299:122621. doi: 10.1016/j.biortech.2019.122621.
14. Jedynak K, Charmas B. Adsorption properties of biochars obtained by KOH activation. Adsorption. 2024;30(2):167-83. doi: 10.1007/s10450-023-00399-7.
15. Das J, Ravishankar H, Lens PN. Biological biogas purification: recent developments, challenges and future prospects. J Environ Manage. 2022;304:114198. doi: 10.1016/j.jenvman.2021.114198.
16. Kulawong S, Artkla R, Sriprapakhan P, Maneechot P. Biogas purification by adsorption of hydrogen sulphide on NaX and Ag-exchanged NaX zeolites. Biomass Bioenergy. 2022;159:106417. doi: 10.1016/j.biombioe.2022.106417.
17. Ángeles Torres R, Marín D, del Rosario Rodero M, Pascual C, González-Sanchez A, de Godos Crespo I, et al. Biogas treatment for H2S, CO2, and other contaminants removal. In: Soreanu G, Dumont É, eds. From Biofiltration to Promising Options in Gaseous Fluxes Biotreatment. Elsevier; 2020. p. 153-76. doi: 10.1016/b978-0-12-819064-7.00008-x.
18. Lin Q, Zhang J, Yin L, Liu H, Zuo W, Tian Y. Relationship between heavy metal consolidation and H2S removal by biochar from microwave pyrolysis of municipal sludge: effect and mechanism. Environ Sci Pollut Res Int. 2021;28(22):27694-702. doi: 10.1007/s11356-021-12631-4.
19. Wang S, Nam H, Lee D, Nam H. H2S gas adsorption study using copper impregnated on KOH activated carbon from coffee residue for indoor air purification. J Environ Chem Eng. 2022;10(6):108797. doi: 10.1016/j.jece.2022.108797.
20. Xia G, Zhou X, Hu J, Sun Z, Yao J, Chen D, et al. Simultaneous removal of carbon disulfide and hydrogen sulfide from viscose fibre waste gas with a biotrickling filter in pilot scale. J Clean Prod. 2019;230:21-8. doi: 10.1016/j.jclepro.2019.05.097.
21. Ma C, Zhao Y, Chen H, Liu Y, Huang R, Pan J. Biochars derived from by-products of microalgae pyrolysis for sorption of gaseous H2S. J Environ Chem Eng. 2022;10(3):107370. doi: 10.1016/j.jece.2022.107370.
22. Zhang X, Lawan I, Danhassan UA, He Y, Qi R, Wu A, et al. Advances in technologies for in situ desulfurization of biogas. In: Li Y, Zhou Y, eds. Advances in Bioenergy. Vol 7. Elsevier; 2022. p. 99-137. doi: 10.1016/bs.aibe.2022.05.001.
23. Zhang Y, Oshita K, Kusakabe T, Takaoka M, Kawasaki Y, Minami D, et al. Simultaneous removal of siloxanes and H2S from biogas using an aerobic biotrickling filter. J Hazard Mater. 2020;391:122187. doi: 10.1016/j.jhazmat.2020.122187.
24. Paulionytė J, Vaiškūnaitė R, Mažeikienė A. Evaluation of sewage sludge biochar use in wastewater treatment from phosphate. Environmental protection technology and management VGTU. 2022. doi: 10.3846/aainz.2022.006.
25. Pudi A, Rezaei M, Signorini V, Andersson MP, Baschetti MG, Mansouri SS. Hydrogen sulfide capture and removal technologies: a comprehensive review of recent developments and emerging trends. Sep Purif Technol. 2022;298:121448. doi: 10.1016/j.seppur.2022.121448.
26. Poser M, Duarte e Silva LR, Peu P, Couvert A, Dumont É. Cellular concrete waste: an efficient new way for H2S removal. Sep Purif Technol. 2023;309:123014. doi: 10.1016/j.seppur.2022.123014.
27. Ying S, Kong X, Cai Z, Man Z, Xin Y, Liu D. Interactions and microbial variations in a biotrickling filter treating low concentrations of hydrogen sulfide and ammonia. Chemosphere. 2020;255:126931. doi: 10.1016/j.chemosphere.2020.126931.
28. Shi M, Xiong W, Zhang X, Ji J, Hu X, Tu Z, et al. Highly efficient and selective H2S capture by task-specific deep eutectic solvents through chemical dual-site absorption. Sep Purif Technol. 2022;283:120167. doi: 10.1016/j.seppur.2021.120167.
29. Konkol D, Popiela E, Skrzypczak D, Izydorczyk G, Mikula K, Moustakas K, et al. Recent innovations in various methods of harmful gases conversion and its mechanism in poultry farms. Environ Res. 2022;214(Pt 2):113825. doi: 10.1016/j.envres.2022.113825.
30. Santos-Clotas E, Cabrera-Codony A, Comas J, Martín MJ. Biogas purification through membrane bioreactors: experimental study on siloxane separation and biodegradation. Sep Purif Technol. 2020;238:116440. doi: 10.1016/j.seppur.2019.116440.
31. Zhang Y, Kawasaki Y, Oshita K, Takaoka M, Minami D, Inoue G, et al. Economic assessment of biogas purification systems for removal of both H2S and siloxane from biogas. Renew Energy. 2021;168:119-30. doi: 10.1016/j.renene.2020.12.058.
32. Choudhury A, Lansing S. Adsorption of hydrogen sulfide in biogas using a novel iron-impregnated biochar scrubbing system. J Environ Chem Eng. 2021;9(1):104837. doi: 10.1016/j.jece.2020.104837.
33. Lee JT, Ok YS, Song S, Dissanayake PD, Tian H, Tio ZK, et al. Biochar utilisation in the anaerobic digestion of food waste for the creation of a circular economy via biogas upgrading and digestate treatment. Bioresour Technol. 2021;333:125190. doi: 10.1016/j.biortech.2021.125190.
34. Bu H, Carvalho G, Huang C, Sharma KR, Yuan Z, Song Y, et al. Evaluation of continuous and intermittent trickling strategies for the removal of hydrogen sulfide in a biotrickling filter. Chemosphere. 2022;291(Pt 1):132723. doi: 10.1016/j.chemosphere.2021.132723.
35. Mohammadi K, Vaiškūnaitė R. Analysis and evaluation of the biogas purification technologies from H2S. Moksl Liet Ateitis. 2023;15:1-9. doi: 10.3846/mla.2023.17242.
36. Su JJ, Hong YY. Removal of hydrogen sulfide using a photocatalytic livestock biogas desulfurizer. Renew Energy. 2020;149:181-8. doi: 10.1016/j.renene.2019.12.068.
37. Alkhatib II, Khalifa O, Bahamon D, Abu-Zahra MR, Vega LF. Sustainability criteria as a game changer in the search for hybrid solvents for CO2 and H2S removal. Sep Purif Technol. 2021;277:119516. doi: 10.1016/j.seppur.2021.119516.
38. Mitchell K, Beesley L, Šípek V, Trakal L. Biochar and its potential to increase water, trace element, and nutrient retention in soils. In: Tsang DC, Ok YS, eds. Biochar in Agriculture for Achieving Sustainable Development Goals. Academic Press; 2022. p. 25-33. doi: 10.1016/b978-0-323-85343-9.00008-2.
39. Wu J, Jiang X, Jin Z, Yang S, Zhang J. The performance and microbial community in a slightly alkaline biotrickling filter for the removal of high concentration H2S from biogas. Chemosphere. 2020;249:126127. doi: 10.1016/j.chemosphere.2020.126127.
40. Huynh Nhut H, Le Thi Thanh V, Tran Le L. Removal of H2S in biogas using biotrickling filter: recent development. Process Saf Environ Prot. 2020;144:297-309. doi: 10.1016/j.

psep.2020.07.011.
41. Talaiekhozani A, Talaei MR, Yazdan M, Mir SM. Investigation of formaldehyde removal from synthetic contaminated air by using human hair. Environ Health Eng Manag. 2016;3(4):191-6. doi: 10.15171/ehem.2016.19.
42. Talaiekhozani A, Eskandari Z, Talaei MR, Salari M. Hydrogen sulfide and organic compounds removal in municipal wastewater using ferrate (VI) and ultraviolet radiation. Environ Health Eng Manag. 2017;4(1):7-14. doi: 10.15171/ehem.2017.02.
43. Jamshidinasirmahale Z, Yazdanbakhsh A, Masoudinejad M, Alavi Bakhtiarvand N. Anaerobic co-digestion of landfill leachate and sewage sludge: determination of the optimal ratio and improvement of digestion by pre-ozonation. Environ Health Eng Manag. 2024;11(1):93-104. doi: 10.34172/ehem.2024.11.
44. Rangabhashiyam S, Lins P, Oliveira L, Sepulveda P, Ighalo JO, Rajapaksha AU, et al. Sewage sludge-derived biochar for the adsorptive removal of wastewater pollutants: a critical review. Environ Pollut. 2022;293:118581. doi: 10.1016/j.envpol.2021.118581.